Nondestructive Resolution of Higher Harmonics of Light-Induced Volume Gratings in PMMA with Cold Neutrons

Frank Havermeyer
Fachbereich Physik, Universität Osnabrück, D-49069 Osnabrück, Germany

Sergei F. Lyuksyutov
Institute of Physics, Ukrainian Academy of Science, 252650 Kiev, Ukraine

Romano A. Rupp
Institut für Experimentalphysik, Universität Wien, A-1090 Wien, Austria

Helmut Eckerlebe, Peter Staron, and Jürgen Vollbrandt
GKSS Forschungszentrum, WFN, Geesthacht, Germany
(Received 12 August 1997)

Illumination of photosensitized (PMMA) with light triggers nonlinear polymerization processes. In this way periodical density structures with nearly 10^4 lines/mm can be generated which are beyond the resolution limit of light-optical investigation methods. We report on the first direct experimental observation of such higher harmonics in deuterated (PMMA) by the nondestructive method of diffraction of neutrons at a wavelength of 1.2 nm. Diffraction efficiency of the second harmonic was found to be 200–500 times weaker than that of the first order. The origin of higher harmonics is attributed to the nonlinearities of the processes of chain growth and of termination. [S0031-9007(98)05599-9]

PACS numbers: 61.12.–q, 42.40.–i, 42.65.–k, 42.70.–a

One of the main advantages of small angle neutron scattering is that both organic (e.g., the structures of ribosomes [1]) and inorganic (e.g., the location of clusters in metals [2]) materials can be studied nondestructively. In this context the discovery of neutron diffraction by photoinduced gratings in polymers [3] has opened several interesting perspectives for polymer research: Diffraction of cold neutrons (with wavelengths from 0.5 to 1.5 nm) provides a very sensitive tool for the study of relaxation processes in nonordered materials including those in polymers [4] and can, in particular, be applied to the study of light-induced processes in polymers.

If PMMA, doped with a photoinitiator, is exposed to a sinusoidally modulated light pattern with period $\Lambda \simeq 2\pi/K$, a mass density grating is created by polymerization which modulates the refractive index for neutrons [5]. Besides the first harmonics such density gratings may also exhibit higher harmonics with spatial frequencies $2K, 3K, \ldots, hK$. This can intuitively be understood from the inherent nonlinearities of chain growth and of termination of the photoinitiated macroradicals which are involved in the formation of the density profile. The modulation of the total number density N, which includes free monomers as well as monomer units bound in polymer chains, is given by $\delta N(x) \simeq \delta N_0 + \delta N_1 \cos(Kx) + \delta N_2 \cos(2Kx) + \cdots$. The amplitude of the refractive index modulation for neutrons is proportional to δN. Its hth Fourier coefficient ($h = 0, 1, \ldots$) can be written as [5] $\delta n_h \simeq (\lambda_n^2/2\pi)\, \bar{b}_c\, \delta N_h$, where λ_n is the wavelength of the neutrons and $\bar{b}_c$ is the coherent scattering length of one monomer unit (95 fm for d-PMMA). As it is possible to reach $\delta N_1 \approx 10^{24}$ m^{-3}, which corresponds to $\delta n_1 \approx 10^{-8}$, gratings can be produced which diffract neutrons with an efficiency of about 71% [6]. An important advantage of PMMA is its high resolution capability which is, e.g., required for the development of interferometers for cold neutrons [7]. Artificial development of density gratings with a profile containing strong higher harmonics permits deflection of neutrons at even larger angles and could appreciably facilitate the development of neutron optical elements. The first experimental demonstration of such higher harmonics of density gratings, which, in principle, cannot be studied by the diffraction of light even though they were induced by light, and the physics of their origin are the subjects of the current Letter.

The preparation of photosensitive d-PMMA samples starts with purification of liquid d-MMA monomer ($C_5O_2D_8$) with a content of 99.8% deuterium. A thermal initiator (to speed up prepolymerization) and a photoinitiator with maximum absorption near 340 nm (to sensitize the samples in the near UV region) are added. All procedures were performed in an argon atmosphere to avoid contact of the distilled monomer with air. The process of prepolymerization of d-PMMA took place for 48 h at a temperature of 50 °C.

Volume gratings with grating spacings of 400, 250, and 204 nm were recorded at room temperature into three d-PMMA samples using a conventional two-wave mixing configuration [8] and an Ar^+ laser at a wavelength of 351 nm. The laser beam was expanded 20 times to fully illuminate the whole area of each sample at a size of 400 mm^2. However, only half of the sample was

 0031-9007/98/80(15)/3272(4)$15.00

illuminated during recording of the grating with $\Lambda = 204$ nm because the angle between the writing beams exceeded 120°. Total intensity of light on the entrance face of the sample was 150 W/m^2, and the recording time was 30 s. The diffraction efficiencies of the samples were determined at 351 nm by diffraction of beams attenuated by a factor of 100 with respect to the writing intensity. For all three samples, diffraction efficiency for light exceeded 50% at the Bragg angle.

The neutron diffraction experiments were performed at the Small Angle Neutron Scattering Facility SANS-2 of the Geesthacht Neutron Facility (GeNF). A neutron beam at a wavelength of 1.2 nm with a wavelength distribution $\Delta\lambda/\lambda \simeq 0.2$ and a lateral divergence of 1.25 mrad was used in our experiments. The distance between the sample and the detector matrix was 21.72 m. The pixel size of the detector matrix was 0.45×0.45 mm^2. The cross section was limited to 10×10 mm^2 by a Cd diaphragm in front of the sample. The neutron flux incident on the entrance face of the sample was 1.45×10^4 s^{-1}. Only 1.08×10^4 neutrons per second were transmitted by the *d*-PMMA samples. After correction for the transmission of the quartz windows, this corresponds to a transmission of 74%. The thickness of the sample is $d \simeq 2.2$ mm which gives a value of 0.14 ± 0.01 mm^{-1} for the primary extinction coefficient.

The diffraction patterns obtained with cold neutrons were particularly interesting for the samples with 250 and 204 nm: distinct second order Bragg peaks corresponding to spacings of 125 ± 5 nm and 102 ± 5 nm were clearly detected for the samples with fundamental spacings of 250 and 204 nm, respectively (Fig. 1). The numbers A_1 and A_2 of neutrons counted by the matrix detector in the spots corresponding to the spatial frequencies K and $2K$ and the number A_{out} of neutrons transmitted by the sample were corrected by subtracting the statistically distributed backgrounds. From these data the diffraction efficiencies $\eta_{1,2}(\theta) = A_{1,2}(\theta)/A_{\text{out}}$ were calculated as a function of the angle θ between the wave vector of the neutron flux and the vector normal to the entrance face of the sample. The neutrons in the $2K$ spots were counted for 5400 and 3600 s for the samples with 204 and 250 nm, respectively, at each angular setting. The diffraction efficiency of the second harmonics as a function of the angle is shown in Fig. 2 for all three samples. The diffraction orders $\pm K$ have an exactly symmetrical location of the peaks and appear with equal magnitude and the same profiles. The widths of the Bragg peaks of the first diffraction order (not shown in Fig. 2) are additionally broadened by $\Delta\theta \simeq 0.2\theta$ which is, e.g., 0.48 mrad for $\Lambda = 204$ nm because of the large dispersion of cold neutrons and by 1.25 mrad because of the angular divergence of the neutron beam. Such large contributions cause the effect of "shifting" of the diffracted spot on the detector matrix when readout is performed with change of the angle. In order to normalize the data with respect to the large spatial and temporal incoherence of the

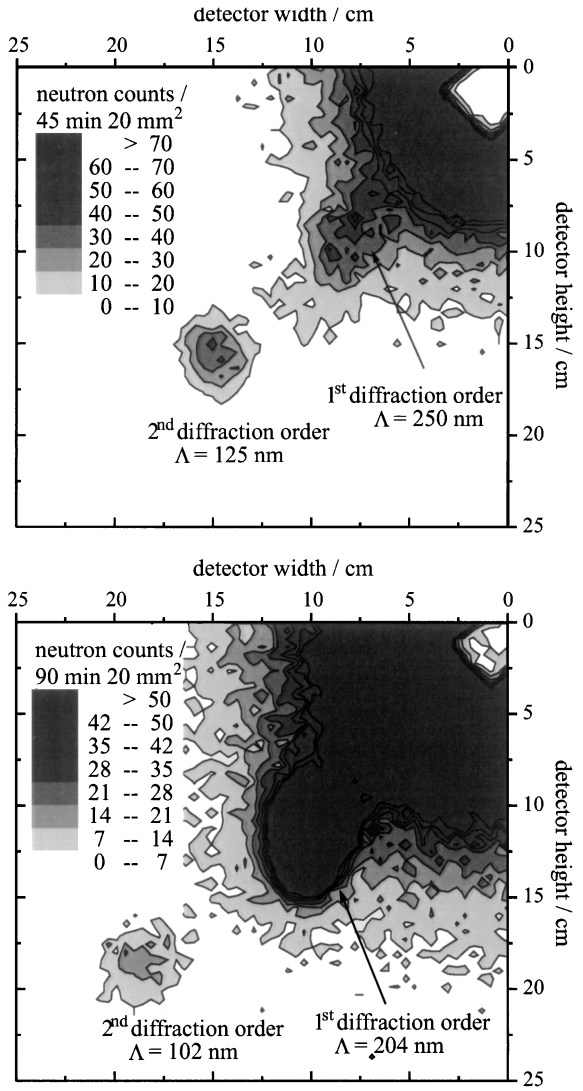

FIG. 1. Distribution of the neutrons on the detector matrix. Bragg spots corresponding to the second ($2K$) harmonics of the light-induced density grating are clearly observed.

neutron beam, the "ideal" diffraction efficiency for a perfect neutron beam $\eta^{id} \simeq \frac{d}{\Lambda}\int_{-\infty}^{+\infty}\eta(\theta)\,d\theta$ was evaluated by integrating the rocking curves [9]. From η_1^{id}, absolute values of the first harmonic of the density amplitude δN_1 of the monomer units were found to be $(12 \pm 2) \times 10^{24}$ m^{-3}, $(2.3 \pm 0.1) \times 10^{24}$ m^{-3}, and $(1.6 \pm 0.2) \times 10^{24}$ m^{-3} for 400, 250, and 204 nm, respectively. The values for diffraction efficiencies of the second harmonics were $\eta_2^{id} \simeq 2.3 \times 10^{-2}$, 1.9×10^{-3}, and 5×10^{-4} resulting in $\delta N_2 = (5 \pm 1) \times 10^{23}$ m^{-3}, $(1.42 \pm 0.05) \times 10^{23}$ m^{-3}, and $(0.73 \pm 0.02) \times 10^{23}$ m^{-3} for 200, 125, and 102 nm, respectively. The origin of the experimentally detected second harmonics can be traced back to the fundamental nonlinearity of the light-induced postpolymerization process of *d*-PMMA. This process starts with the decay of a molecule of the photoinitiator S with a probability $k_s I$ into two radical molecules R_0^* under the

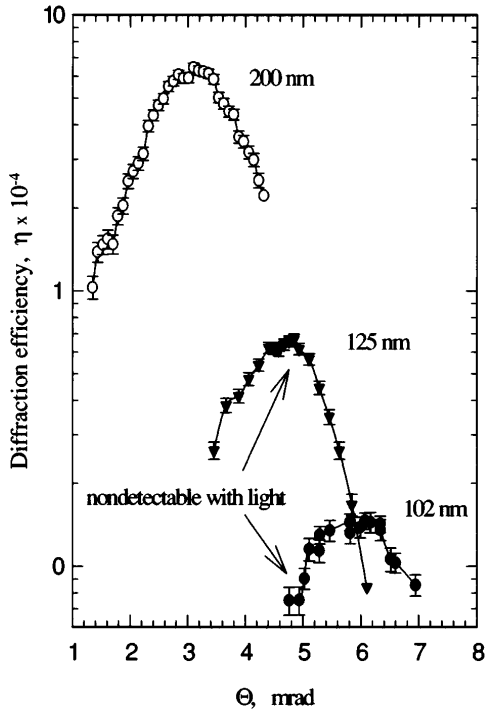

FIG. 2. Diffraction efficiency of the second harmonics of the density grating in *d*-PMMA as a function of the angle of incidence.

action of light with intensity I during exposure time t,

$$S \xrightarrow{k_s I} 2R_0^* . \tag{1}$$

The radicals grow by adding free monomers with a probability k_p to the chain. This process results in the creation of macroradicals R_n^* with different lengths depending on the number of monomer units n in the radical chain,

$$R_n^* + M \xrightarrow{k_p} R_{n+1}^*, \qquad n = 0, 1 \ldots . \tag{2}$$

We assume here that the probabilities of the chemical reactions are independent from the chain length of the radical which is plausible above a certain chain length. By the coupling of the two free radical electrons the interacting radicals can recombine to one polymer molecule with the sum of the monomer units [recombination of radicals—Eq. (3)]. The second process of termination is a hydrogen transfer reaction and results in two polymer molecules [disproportionation—Eq. (4)],

$$R_n^* + R_m^* \xrightarrow{k_t} P_{n+m} , \tag{3}$$

$$R_n^* + R_m^* \xrightarrow{k_t} P_n + P_m . \tag{4}$$

For simplicity, we assume here that the probability k_t of termination by recombination and disproportionation is the same, and we do not distinguish between radical and polymer chains of different lengths, therefore introducing the total number density: $N_R = \sum_{n=0}^{\infty} N_{R_n}$ of radicals. Now we are able to write the kinetic equations considering a one-dimensional model which describes the four main processes: reaction diffusion of the radical position, diffusion of monomer units, chain growth, and termination of the radicals. Reaction diffusion of radicals is the migration of the σ electrons during chain growth while the diffusion of monomers is a random walk of the monomer molecules. The current density of monomer units and of the radical molecules can be written as $J_{M,R} \simeq -D_{M,R} dN_{M,R}/dx$. Here D_M and D_R are diffusion coefficients for monomers and the reaction diffusion constants for radical (chains). By using the continuity equation for monomers and radicals, we obtain the following equations for the number density of radicals N_R and monomers N_M:

$$-D_R \frac{\partial^2 N_R}{\partial x^2} + k_t N_R^2 = -\frac{\partial N_R}{\partial t} , \tag{5}$$

$$-D_M \frac{\partial^2 N_M}{\partial x^2} + k_p N_R N_M = -\frac{\partial N_M}{\partial t} . \tag{6}$$

A similar model has been studied by Marotz [10]. However, the appearance of higher harmonics in the model was entirely attributed to the consequence of overexposure in the photopolymerization process. This does not apply to our experiments, because the exposure time was so short that such a source of nonlinearity can be excluded. In our model the nonlinearity is related to the chemical processes during postpolymerization such as termination of radicals [Eq. (5)].

After a brief exposure to light, the initial distribution of radicals at the time $t = 0$ can be written as $N_R(0) = \bar{N}_R(0)[1 + a\cos(Kx)]$, where $a < 1$, and $\bar{N}_R$ is the average of the initial distribution of radicals. With this starting condition, we solved Eqs. (5) and (6) numerically. By taking the values of the chemical constants for PMMA from the literature [11], we originally studied the behavior up to the second harmonics, considering $\delta N_M = \frac{1}{2}\delta N_{M,0} + \delta N_{M,1}\cos(Kx) + \delta N_{M,2}\cos(2Kx)$. This assumption is based on a Fourier analysis of the function N_M and also on the experimental observation that only two harmonics, K and $2K$, of the density grating are detectable in PMMA. To fit our experimental data with calculations, we selected the following set of parameters: $k_p = 0.57 \times 10^{-31}\ \mathrm{m^3\,s^{-1}}$, $k_t = 0.51 \times 10^{-28}\ \mathrm{m^3\,s^{-1}}$, and $\bar{N}_{M,0} = 11.88 \times 10^{26}\ \mathrm{m^{-3}}$. We calculated the starting average value of the density of radicals by using experimental values of the absorption coefficient and the concentration $6 \times 10^{23}\ \mathrm{m^{-3}}$ of the photoinitiator. The time of postpolymerization was 2.6×10^6 s and the contrast a of the grating was 0.9.

However, to obtain coincidence between experiment and numerical calculations we used a value of k_p which was approximately 35 times larger than that in [11]. We found that for a broad range of diffusion constants (D_M, $D_R \ll 10^{-23}\ \mathrm{m^2\,s^{-1}}$), the effect of diffusion on the solution for N_M can be neglected. Curve No. 2 of Fig. 3 shows a numerical solution for N_M including the second

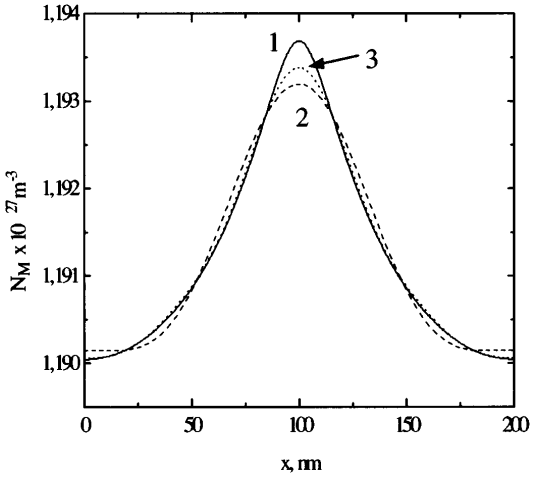

FIG. 3. The number density profile for the monomer concentration. Curve No. 1: analytical solution with the presence of all harmonics; curves No. 2 and No. 3: numerical solution for the first two and four harmonics, respectively, including the effect of diffusion.

harmonics. For comparison, curve No. 3 shows the effect of additional contributions up to the fourth harmonics.

The solution $N_M(t) = N_M(0)[1 + N_R(0)k_t t]^{-k_p/k_t}$ of Eqs. (5) and (6) for the case of neglected diffusion can be obtained by straightforward calculation. Here $N_M(0)$ and $N_R(0)$ denote the initial concentrations for monomer and radical molecules. This solution is shown in Fig. 3 for the selected values of the chemical constants as curve No. 1. As can be seen, the effect of the third and fourth harmonics are still needed to obtain good coincidence between numerical and analytical solutions. The fact that we have not yet experimentally observed the components $3K$ and $4K$ can be explained by the fact that the diffraction efficiency $\eta_h \propto \delta N_{M,h}^2$ (for small efficiencies) decreases quadratically with the hth harmonics $\delta N_{M,h}$ of the density modulation.

The limiting cases $k_p \gg k_t$ and $k_t \gg k_p$ of this solution approach $N_M(t) = N_M(0)\exp[-k_p N_R(0)t]$ and $N_M(t) = N_M(0)\{1 - (k_p/k_t)\ln[1 + k_t N_R(0)t]\}$, respectively. In the first case, the nonlinearity is a consequence of the chain growth nonlinearity ($\propto N_R Nm$) and in the second one of the chain termination nonlinearity ($\propto N_R^2$). From the considerations presented so far, we expect that valuable information on the photopolymerization process might be obtained in future experiments by simultaneous measurements of the time dependence of the first and second order diffraction with light and neutron waves from light-induced gratings.

Light absorption of deuterated PMMA doped with photoinitiator steeply rises below 320 nm, where the refractive index attains the value of $n = 1.523$ [12]. Therefore gratings with spacings below $\Lambda = \lambda/2n = 105$ nm cannot, on principle, be detected by light diffraction experiments even at the limiting wavelength 320 nm. If the sample shape and/or the direction of the grating vector only permits readout under transmission (Laue) conditions, then the practical limit is even higher, namely, $\Lambda = \lambda/2 = 160$ nm. Therefore our experiment demonstrates for the first time that gratings arising from light-triggered nonlinear processes can be studied by neutron diffraction methods, when they cannot, in principle, be detected by optical means because of the onset of the fundamental optical absorption. By this we established a new technique for the study of nonlinear processes which are needed for the nanostructurization of matter, a topic which is of high importance, e.g., for the design of interferometers for cold and ultracold neutrons [7]. In addition, we want to stress that our method clearly allows us to distinguish between linear and nonlinear processes with first and second order kinetics, respectively. We obtained clear evidence that nonlinear chemical processes play an important role in the photopolymerization down to a spatial frequency $K = 3.08 \times 10^{-2}$ nm^{-1}.

In summary, we experimentally observed a profile of the density grating in *d*-PMMA with a characteristic period near 100 nm. It is not possible to resolve such holographic structures with existing optical methods. To our knowledge, this is the first report on the possibility of directly observing higher harmonics of density gratings in polymer materials at a primary grating spacing of less than 300 nm.

This work was funded by the BMBF of the FRG (Project No. RU11.12K) and supported by the GKSS.

[1] H. B. Stuhrmann, Phys. Scr. **T49**, 644 (1993).
[2] G. Kostorz, J. Appl. Cryst. **24**, 444 (1991).
[3] R. A. Rupp, J. Hehmann, R. Matull, and K. Ibel, Phys. Rev. Lett. **64**, 301 (1990).
[4] R. Matull, P. Eschkötter, R. A. Rupp, and K. Ibel, Europhys. Lett. **15**, 133 (1991).
[5] H. Dachs, *Topics in Current Physics—Neutron Diffraction* (Springer-Verlag, Berlin, 1978).
[6] R. A. Rupp, R. Heintzmann, S. Breer, and U. Schellhorn, Institute Laue Langevin Experimental Report No. 5-16-237, 1995.
[7] U. Schellhorn, R. A. Rupp, S. Breer, and R. P. May, Physica (Amsterdam) **234–236B**, 1068 (1997).
[8] N. Kukhtarev, V. Markov, S. Odulov, M. Soskin, and V. Vinetskii, Ferroelectrics **22**, 949 (1979).
[9] R. A. Rupp, U. Hellwig, U. Schellhorn, J. Kohlbrecher, A. Wiedenmann, and J. Woods, Polymer **10**, 2299 (1997); see also U. Schellhorn, Dissertation, University of Osnabrück, 1997.
[10] J. Marotz, Appl. Phys. B **37**, 181 (1985).
[11] H.-J. Cantow and M. Stickler, Makromol. Chem. **184**, 2563 (1983).
[12] F. Mesegner and C. Sanchez, J. Mater. Sci. **15**, 53 (1980).